

**STUDY OF COLOR MAGNITUDE DIAGRAM
FOR OPEN CLUSTERS**

**By
R.K.B.D.M.S.D.K.Ketakella
(08/AS/074)**

Final year project report submitted in partial fulfillment of requirement for the degree
of Bachelor of Sciences (Special) Degree
In
Applied Physics.

Department of Physical Sciences and Technology
Faculty of Applied Sciences
Sabaragamuwa University of Sri Lanka
Belihuloya



Department of Physical Sciences and Technology
Faculty of Applied Sciences
Sabaragamuwa University of Sri Lanka
Belihuloya

Final Year Project Report

Affectionately dedicated to my parents, teachers
and whoever helped me in my life.

DECLARATION

I carried out the work described in this thesis at the Arthur C. Clarke Institute for Modern Technologies (ACCIMT), Katubadda, Moratuwa, under the supervision of Mr. Janaka Adassuriya, research scientist at Arthur C. Clarke Institute for Modern Technology. The contents of this thesis have not been submitted to any other university or degree program .

R.K.B.D.M.S.D.K.Ketakella

08/AS/074

EP733

.....

Date

.....

Signature

Certificate of Approval

We hereby declare that this Research report is from the student's own work and effort, and all other sources of information used have been acknowledged. This research report has been submitted with our approval.

Read by,

- **Internal Supervisor:**

Prof. IndralK. Perera
Sabaragamuwa University of Sri Lanka,
Belihuloya
Sri Lanka
T'phone: 94 - 45 - 2280285
94 - 71 - 8329359
94 - 11 - 2813013
Email: indral@ac.lk

.....

Signature

.....

Date

- **External Supervisor:**

JanakaAdassuriya
Research Scientist,
Space Applications Division,
Artrur C. Clarke Institute for Modern Technologies,
Katubedda,
Moratuwa
Tel:+94112651566
Email: adassuriya@accmt.ac.lk

.....

Signature

.....

Date

Head of the Department

Dr. Lasantha Aponso

Head of Dept. Physical Sciences & Technology,

Faculty of Applied Sciences,

Sabaragamuwa University of Sri Lanka,

Belihuloya.

T.P: +94718098824

.....

Signature

.....

Date

ACKNOWLEDGEMENT

I have done my best in completing this project. However, it would not have been possible without the kind support and help of many individuals. I would like to extend my sincere gratitude to all of them.

My deepest sense of gratitude to my internal supervisor Prof. Indral K. Perera of the Sabaragamuwa University of Sri Lanka, for providing opportunity, guidance, advice, all encouragement, spending lot of valuable time and endless help for the success of this research.

I am specially thankful to Dr. Janaka Adassuriya, Research Scientist, Space applications Division, Arthur C. Clarke Institute for Modern Technologies (ACCIMT), who was my external supervisor, for providing an opportunity for me to conduct this study, his guidance, the assistance and all the encouragement he extended to me to complete the research project successfully.

The Director of Arthur C Clarke Institute for Modern Technologies (ACCIMT), monitored my progress and arranged all facilities to make my life at the ACCIMT much easier. I take this opportunity to appreciate his contribution to complete my project. My grateful thanks are also due to Mr. Sarajh Gunasekara at Arthur C. Clarke Institute for Modern Technology at Katubadda.

And I am thankful to all academic and nonacademic staff of the Department of Physical Sciences and Technology, Faculty of Applied Sciences, Sabaragamuwa University of Sri Lanka, for helping me during the study period.

The success of my project also depended on the encouragement and guidance of many others. I take this opportunity to express my gratitude to all those people who have been instrumental in extending their assistance that enabled the successful completion of this project.

Finally I would like to extend my special thanks to all of my family members and also to my dearest friends who extended their support in many ways.

ABSTRACT

Open clusters are relatively young stellar objects and are located in the plane of the disk of our galaxy. Typically, they contain a few thousands of stars and are gravitationally bound to each other, though at a lower magnitude, thus, making them easier to resolve even in a small telescope. The stars spend their lifetime in main sequence because open clusters tend to be dispersed before most of their stars reach the end of their lives; the light from them being dominated by the young, hot blue stars. These stars are the most massive, and have the shortest lives of a few tens of millions of years. The older open clusters tend to contain more yellow stars. Some open clusters contain hot blue stars which seem to be much younger than the rest of the cluster.

The aim of this project was to construct the Color-Magnitude diagram (CMD) of selected open clusters and identify the different types of stars in these clusters and to estimate the distance modulus. The images of open clusters, NGC663, NGC1513, and NGC1528 have been observed using the 50 cm reflective telescope at Mount Abu observatory, Rajasthan, India during the period of 09th to 12th December 2013. The images were taken through the B, V and R filters, with each frame been exposed for 5 seconds. For standardization purposes, Landolt standard stars were also observed during the same nights the other observations were made.

Initially the IRAF *daofind* and *phot* packages were used to determine the instrumental magnitudes of the stars for each filter. After photometric data have been properly extracted, it was converted into the standard system that finally allowed the construction of the color-magnitude diagram.

The Color-Magnitude diagram of NGC663 showed a feeble main sequence pattern and also the suspected red giant stars. The CMD diagram of NGC1528 has strong main sequence branch with a prominent turn off point. The three stars (with RA and DEC values: 04:15:19.59, 51:14:23.03; 04:15:09.98, 51:11:40.98 & 04:15:46.57, 51:10:55.01) in NGC1528, which deviated from the main sequence, moving towards the red side can be confirmed as red giant stars. In order to estimate the distance modulus, the CMD diagram of open cluster NGC1513 was shifted to the standard CMD for nearby stars. Hence the distance modulus, $m_V - M_V$, is estimated to be 10.750 ± 0.995 [mag] in magnitude scale for the open cluster NGC1513.

TABLE OF CONTENT

| | |
|---|------|
| Declaration..... | iv |
| Certificate of approval..... | v |
| Acknowledgments..... | vii |
| Abstract | viii |
| Table of content..... | ix |
| List of figures..... | xi |
| List of table | xii |
| Abbreviations and symbols..... | xiii |
| Chapter 01 Introduction..... | 1 |
| 1.1.Star cluster | 1 |
| 1.1.1.Open cluster | 2 |
| 1.1.2.Globular cluster..... | 3 |
| 1.2.Color magnitude diagram..... | 4 |
| 1.2.1.Main sequence star..... | 4 |
| 1.2.2.Red giant stars..... | 5 |
| 1.2.3.White dwarfs | 5 |
| 1.2.4.Blue stragglers..... | 5 |
| 1.3.Distance modulus | 6 |
| 1.4.Instrumental magnitude..... | 6 |
| 1.5.Absolute magnitude..... | 6 |
| 1.6.Transformation of pixel coordinates to world coordinates..... | 7 |
| 1.7.The pixel coordinates..... | 7 |
| 1.8.The world coordinate system..... | 7 |
| 1.9.The Right ascension and the Declination..... | 8 |
| 1.10. IRAF software..... | 8 |
| 1.10.1. FITS file..... | 9 |
| 1.10.2. The WCS tool..... | 9 |
| CHAPTER 02 LITERATURE REVIEW..... | 10 |
| 2.1. Color magnitude diagram..... | 10 |
| 2.1.1. Formation of Blue Stragglers..... | 12 |
| 2.1.2. Evolution of red giant branch stars..... | 12 |

| | |
|--|----|
| 2.1.3. Formation of main sequence stars..... | 12 |
| 2.2. The age of clusters | 13 |
| 2.3. Distance modulus..... | 14 |
| 2.4. Standardization | 16 |
| CHAPTER 03 MATERIAL AND ETHODOLOGY..... | 18 |
| 3.1. Material..... | 18 |
| 3.1.1. Optical system | 19 |
| 3.1.2. Primary mirror..... | 19 |
| 3.1.3. Secondary mirror..... | 20 |
| 3.1.4. Lens group..... | 20 |
| 3.1.5. Standard features..... | 20 |
| 3.1.6. CCD camera..... | 21 |
| 3.1.6.1. Function of the CCD camera..... | 21 |
| 3.1.6.2. Quantum efficiency of the CCD camera..... | 21 |
| 3.1.6.3. Photon noise..... | 22 |
| 3.1.6.4. Thermal noise..... | 22 |
| 3.1.6.5. Read out noise..... | 22 |
| 3.1.6.6. Quantized noise..... | 23 |
| 3.1.6.7. Sensitivity variation noise | 23 |
| 3.1.7. Specification of ANDOR CCD camera..... | 23 |
| 3.2. Methodology..... | 23 |
| CHAPTER 04 RESULT AND DISCUSSION..... | 33 |
| 4.1. Results..... | 33 |
| 4.1.1. NGC 663..... | 33 |
| 4.1.2. NGC 1513..... | 35 |
| 4.1.3. NGC 1528..... | 38 |
| 4.2. Discussion..... | 38 |
| CHAPTER 05 CONCLUSION..... | 41 |
| REFERENCES..... | 42 |
| Appendices..... | 43 |

LIST OF FIGURE

| | |
|---|----|
| Figure 1.1 Open cluster M63 | 2 |
| Figure 1.2 globular cluster..... | 3 |
| Figure 1.3 Typical CMD diagram..... | 4 |
| Figure 1.4 The Right Ascension & Declination..... | 8 |
| Figure 3.1 20 inch reflector telescope..... | 18 |
| Figure 3.2 ANDOR ixon ultra camera..... | 23 |
| Figure 3.3 Cluster image..... | 24 |
| Figure 3.4 Flat field image..... | 24 |
| Figure 3.5 image categorize code..... | 25 |
| Figure 3.6 Parameters for imshift..... | 26 |
| Figure 3.7 Parameters for imcombine..... | 27 |
| Figure 3.8 Parameters for setairmass..... | 28 |
| Figure 3.9 Parameters for daofind..... | 29 |
| Figure 3.10 image of selected stars using daofind, tvmmark..... | 30 |
| Figure 3.11 Output of fitting graph by IRAF..... | 22 |
| Figure 4.1 CMD diagram of NGC 663..... | 34 |
| Figure 4.2 CMD diagram of NGC 663 | 35 |
| Figure 4.3 CMD diagram of NGC 1513 | 37 |
| Figure 4.4 CMD diagram of NGC 1513 | 37 |
| Figure 4.5 CMD diagram of NGC 1528 | 40 |
| Figure 4.6 CMD diagram of NGC 1528 | 40 |

LIST OF TABLES

| | |
|--|----|
| Table 3.1 Features of optical system..... | 19 |
| Table 3.2 features of primary mirror..... | 19 |
| Table 3.3 Features of secondary mirror..... | 20 |
| Table 3.4 Features of lens group..... | 20 |
| Table 3.5 Standard features..... | 20 |
| Table 3.6 Specification of ANDOR CCD camera..... | 23 |
| Table 4.1 Observation airmass of the NGC 663 open cluster..... | 33 |
| Table 4.2 Instrumental magnitudes..... | 33 |
| Table 4.3 Standard solution of NGC 663..... | 33 |
| Table 4.4 Absolute magnitude and apparent magnitude | 34 |
| Table 4.5 Observation airmass of the NGC 1513 open cluster..... | 35 |
| Table 4.6 Instrumental magnitudes of NGC 1513..... | 35 |
| Table 4.7 Standard solution for NGC 1513..... | 36 |
| Table 4.8 Absolute magnitude and apparent magnitude..... | 36 |
| Table 4.9 Selected Absolute and apparent magnitude for distance modulus..... | 38 |
| Table 4.10 Observation airmass of the NGC 1528 | 38 |
| Table 4.11 Instrumental magnitude of NGC 1528..... | 38 |
| Table 4.12 Standards solution of NGC 1528..... | 39 |
| Table 4.13 The apparent magnitude of NGC 1528..... | 39 |

ABBREVIATIONS AND SYMBOLS

| | |
|----------|--|
| FWHM | : Full Width at Half Maxima |
| CCD | : Charge Couple Device |
| IRAF | : Image Reduction and Analyzing Facility |
| CMD | : Color-Magnitude diagram |
| NGC | : National Galactic Cluster |
| BSs | : Blue Stragglers |
| WCS | : World Coordinate System |
| RA | : Right Ascension |
| DEC | : Declination |
| NOAO | : National Optical Astronomy Observatory |
| HR | : Hertzsprung–Russell |
| ZAMS | : Zero Age Main Sequence |
| CDK | : Corrected Dall-Kirkham |
| ST | : Sidereal Time |
| UT | : Universal Time |
| U filter | : Ultraviolet filter |
| B filter | : Blue filter |
| V filter | : Visible filter |
| R filter | : Red filter |
| I filter | : Infrared filter |

CHAPTER 01 INTRODUCTION

The aim of this project was to construct a color-magnitude diagram for selected open clusters and identify the different types of stars in these clusters and estimate the distance modulus. The images of open clusters (NGC663, NGC1513, and NGC1528) were observed using the CDK 20 inch plane wave telescope at Mount Abu observatory, Rajasthan, India, during the period 09th to 12th December 2013. The images were taken through the B, V and R filters, with each frame been exposed for 5 seconds. For standardization, Landolt standard stars were also observed during the same nights the above readings were taken

Initially the IRAF *daofind* and *phot* packages were used to determine the instrumental magnitudes of the stars for each filter. After photometric data have been properly extracted, it was converted into the standard system that finally allowed the construction of the color-magnitude diagram.

The Color-Magnitude diagram (CMD) of NGC663 shows a weak main sequence pattern with suspected red giant stars and white dwarfs. The CMD diagram of NGC1528 shows a strong main sequence branch and in addition the turn off point was also observed to be present. The CMD of NGC1513 has a main sequence pattern and the distance modulus for NGC1513, was estimated to be 10.75 ± 0.995 [mag].

1.1. Star Cluster

When stars are born they develop from large clouds of molecular gas. This means that they form in groups or clusters, since molecular clouds are composed of hundreds of solar masses of material. After the remnant gas is heated and is blown away, the stars collect together by gravity. During the exchange of energy between the stars, some stars reach escape velocity from the proto cluster and become runaway stars. The rest become gravitationally bound, meaning they will exist as a collection orbiting each other forever.

Star clusters or star clouds are groups of stars. There are two types of star clusters,

- Open Clusters and
- Globular Clusters

1.1.1. Open Clusters



Figure 1.1 : Open cluster M63

An open cluster is a group of up to a few thousand stars that were formed from the same giant molecular cloud and have roughly the same age. More than 1,100 open clusters have been discovered within the Milky Way Galaxy, and many more are thought to exist. They are loosely bound to each other by mutual gravitational attraction and become disrupted by close encounters with other clusters and clouds of gas as they orbit the galactic center, resulting in a migration to the main body of the galaxy as well as a loss of cluster members through internal close encounters. Open clusters generally survive for a few hundred million years. In contrast, the more massive globular clusters of stars exert a stronger gravitational attraction on their members, and can survive for many billions of years. Open clusters have been found only in spiral and irregular galaxies, in which active star formation is occurring.

Open clusters are key objects in the study of stellar evolution. Because the cluster members are of similar age and chemical composition, the effects of other stellar properties are more easily determined than they are for isolated stars. A number of open clusters, such as the Pleiades, Hyades or the Alpha Persia Cluster are visible for the naked eye. Some others, such as the Double Cluster, are barely perceptible without instruments, while many more can be seen using binoculars or telescopes.

1.1.2 Globular Clusters



Figure 1.2 : Globular cluster

A globular cluster is a spherical collection of stars that orbits a galactic core as a satellite. Globular clusters are very tightly bound by gravity, which gives them their spherical shapes and relatively high stellar densities toward their centers. The name of this category of star cluster is derived from the Latin *globules* a small sphere. A globular cluster is sometimes known more simply as a globular.

Globular clusters, which are found in the halo of a galaxy, contain considerably more stars and are much older than the less dense galactic, which are found in the disk. Globular clusters are fairly common; there are about 150 to 158 currently known globular clusters in the Milky Way, with perhaps 10 to 20 more still undiscovered. Large galaxies can have more: Andromeda, for instance, may have as many as 500. Some giant elliptical galaxies, particularly those at the centers of galaxy clusters, orbit the galaxy with the path having large radii, 40 kilo parsecs (approximately 131,000 light-years) or more. Every galaxy of sufficient mass in the Local Group has an associated group of globular clusters, and almost every large galaxy surveyed has been found to possess a system of globular clusters. The Sagittarius Dwarf galaxy and the disputed Canes Major Dwarf galaxy appear to be in the process of donating their associated globular clusters (such as Palomar 12) to the Milky Way. This demonstrates how many of this galaxy's globular clusters might have been acquired in the past.

Although it appears that globular clusters contain some of the first stars to be produced in the galaxy, their origins and their role in galactic evolution are still

unclear. It does appear clear that globular clusters are significantly different from dwarf elliptical galaxies and were formed as part of the star formation of the parent galaxy rather than as a separate galaxy. However, recent conjectures by astronomers suggest that globular clusters and dwarf spheroidals may not be clearly separate and distinct types of objects.

1.2. Color Magnitude Diagram

Photometry can be defined as the determination of the amount and temporal nature of the flux emitted by an astronomical object as a function of wavelength (Howell, 2000). By taking images of a star at different wavelengths, and then analyzing the intensity in each image, one can determine each star's magnitude, color, and spectral class. By imaging the stars in a cluster, whether it's open or globular, one can determine the cluster's approximate age and evolution.

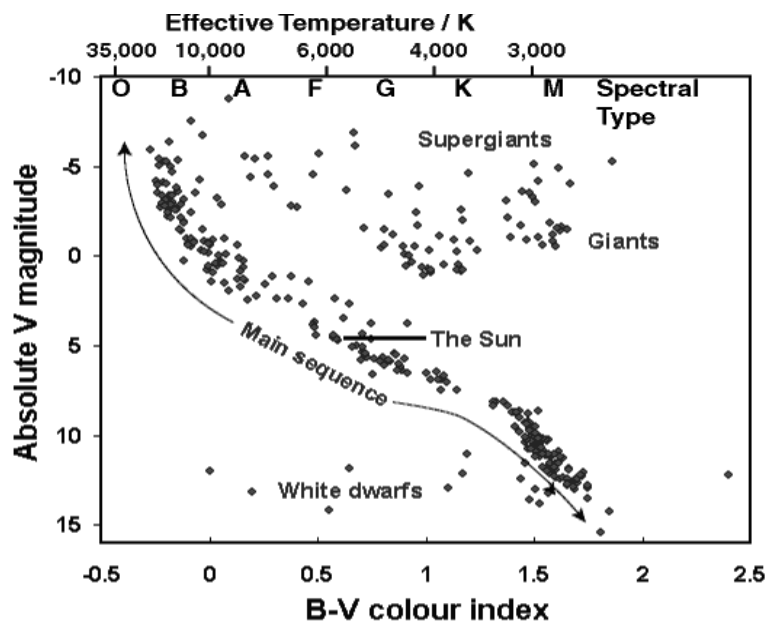


Figure 1.3 : Typical CMD diagram

1.2.1. Main Sequence Stars

A star is said to be born once nuclear fusion commences in its core. At this point it is, considered a main sequence star, regardless of mass. This is where the majority of a star's life is spent. Our Sun has been on the main sequence for about 5 billion years, and will persist for another 5 billion years or so before it transits to become a Red Giant Star.

1.2.2. Red Giant Stars

Once a star has used up all of its hydrogen fuel in its core it transits off the main sequence and becomes a red giant. Depending on the mass of the star it can oscillate between various states before ultimately becoming a white dwarf, neutron star or black hole. One of our nearest neighbors (galactically speaking), Betelgeuse is currently in its red giant phase and is expected to convert to a supernova at any time.

1.2.3. White Dwarfs

When low-mass stars, like our Sun, reach the end of their lives they enter the red giant phase. But the outward radiation pressure overwhelms the gravitational pressure and the star expands farther and farther out into space. Eventually, the outer envelope of the star begins to merge with interstellar space and all that is left behind is the remnant of the star's core. This core is a smoldering ball of carbon and other various elements that glows as it cools. While often referred to as a star, a white dwarf is not technically a star as it does not undergo nuclear fusion. Rather it is a stellar *remnant*, like a black hole or neutron star. Eventually it is this type of object that will be the sole remains of our Sun billions of years from now.

1.2.4. Blue Stragglers

Blue stragglers (BSS) are main sequence stars in open or globular clusters that are more luminous and bluer than the stars at the main-sequence turn-off point for the cluster. Blue stragglers were first discovered by Allan Sandage in 1953 while performing photometry of the stars in the globular cluster. Standard theories of stellar evolution hold that the position of a star on the Hertzsprung–Russell diagram should be determined almost entirely by the initial mass of the star and its age. In a cluster, stars that are all formed at approximately the same time, and thus in an H–R diagram for a cluster, all stars should lie along a clearly defined curve set by the age of the cluster, with the positions of individual stars on that curve determined solely by their initial mass. With masses two to three times that of the rest of the main-sequence cluster stars, blue stragglers seem to be exceptions to this rule. The resolution of this problem is likely related to interactions between two or more stars in the dense confines of the clusters in which blue stragglers are found.

1.3. Distance Modulus

The ‘distance modulus’ is the difference between the apparent magnitude and absolute magnitude of a celestial object ($m - M$), and provides a measure of the distance to the object

$$\text{Distance modulus} = m_v - M_v \longrightarrow (1)$$

1.4. Instrumental Magnitude

Instrumental magnitude refers to an un-calibrated apparent magnitude, and, like its counterpart, refers to the brightness of an astronomical object seen by an observer on Earth, but unlike its counterpart, it is only useful in relative comparisons to other astronomical objects in the same image (assuming the photometric calibration does not spatially vary across the image; in the case of images from the Palomar Transient Factory, the absolute photometric calibration involves a zero point that varies over the image by up to 0.16 magnitudes to make a required illumination correction^[1]). The instrumental magnitude is defined in various ways, and so when working with instrumental magnitudes, it is important to know how they are defined. The most basic definition of instrumental magnitude, m , is given by

$$m = -2.5 \log_{10} (f) \longrightarrow (2)$$

where f is the intensity of the source object in known physical units.

1.5. Absolute Magnitude

Absolute magnitude is the measure of a celestial object's intrinsic brightness. It is the hypothetical apparent magnitude of an object's brightness at a standard luminosity distance of exactly 10.0 parsecs or about 32.6 light years from the observer, assuming that there is no astronomical extinction of starlight. This allows the true energy output of astronomical objects to be compared without regard to their variable distances. As with all astronomical magnitudes, the absolute magnitude can be specified for different wavelength intervals; for stars the most commonly quoted absolute magnitude is the absolute visual magnitude, which is the absolute magnitude in the visual (V) band of the UBV system. Also commonly used is the absolute bolometric magnitude, which is the total luminosity expressed in magnitude units; it takes into account energy radiated at all wavelengths, whether observed or not.

1.6. Transformation of Pixel Coordinates To World Coordinates

To transform the pixel coordinates (physical coordinates) of an astronomical image to the sky coordinates (World Coordinates) a software package called “IMWCS”, a layered package in astronomical image processing software (IRAF) is used. The raw images taken through the CCD camera is converted to the FITS image format which is recognized by the IRAF using the tasks provided in IRAF. Each FITS image has a header and pixel information. Image header has several key words which provide vital information about the image. When IMWCS tasks are executed on the FITS image, the relationship between pixel coordinates in the image and sky coordinates are written to the keywords in the header of a FITS image (WCS) World Coordinate System . IRAF display tasks use these WCS keywords in the image header to display the RA (Right Ascension) and DEC (Declination) coordinates of the pixels in the image.

1.7. The Pixel Coordinates

In digital cameras such as CCD camera pixel information of an image is stored in an array with the pixel coordinates and their corresponding pixel values (Analog to digital units-ADU). Pixel coordinates is the normal coordinate system which is used to define its position in 2-dimensional space in the x direction and the y direction. Each image is referred to in terms of two-coordinates, with the x- and y-coordinates of the stars and the asteroid being measured. Thus, it should be performed to convert the measurements to right ascension and declination which is referred to as the world coordinate system.

1.8. The World Coordinate System

In order to get the precise position of objects observed in the night sky, modern astronomy used the World Coordinate System which means coordinates that serve to locate a measurement in some multi-dimensional parametric space. Under the world coordinate system, the Right Ascension and Declination are used in astronomy to determine the location of stars, planets and other objects in the night sky. They are similar to the system of longitude and latitude used to locate places on Earth. In order to understand this system, we have to first understand the concept of the celestial sphere, vernal equinox and also longitude and latitude.

1.9. The Right Ascension & the Declination(RA, DEC)

The right ascension of a point is the angular distance measured eastward along the celestial equator between vernal equinox and the hour circle intersecting the point. It is measured in hours (h), minutes (m) and seconds (s) and is similar to longitude on Earth. As the Earth rotates, stars appear to rise in the East and set in the West just like the Sun.

The declination of a point is the angular distance above or below the celestial equator. It is measured in degrees, minutes, and seconds from -90° to $+90^{\circ}$ with 0° being on the celestial equator. Negative degrees indicate that the point is south of the celestial equator, while positive degrees indicate that it is in the north of the celestial equator. Declination (Dec) is measured in degrees ($^{\circ}$), arc-minutes ($'$) and arc-seconds ($''$), and is similar to latitude on Earth.

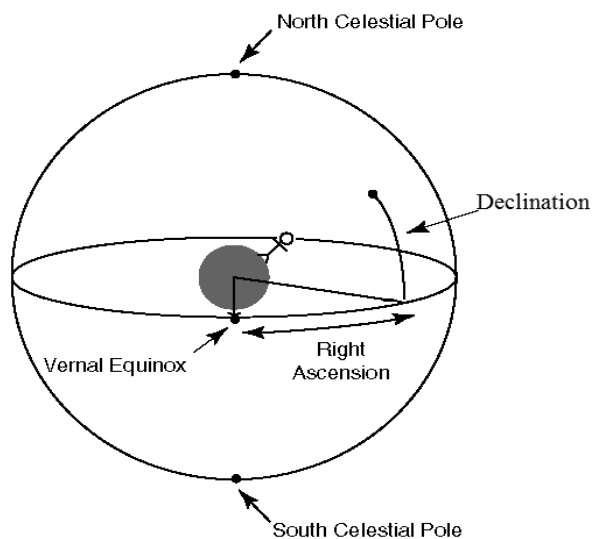


Figure 1.4 : The Right Ascension & Declination

1.10. IRAF Software

IRAF (Image Reduction and Analysis Facility) is a collection of software written at the National Optical Astronomy Observatory (NOAO) geared towards the reduction of astronomical images in pixel array form. This is primarily data taken from imaging array detectors such as CCDs. It is available for all major operating systems for mainframes and desktop computers. Although written for UNIX-like operating systems, use on Microsoft Windows is made possible by Cygwin.

1.10.1. FITS File

FITS or Flexible Image Transport System is the data format most widely used within astronomy for transporting, analyzing and archiving scientific data files. It was developed by the astronomer Wells in the late 1970's. FITS is much more than just another image format such as JPG or GIF and primarily designed to store scientific data sets consisting of multi-dimensional image and 2-dimensional tables organized into rows and columns of information. In the past decade FITS has also become the standard format for online data that can be directly read and written by data analysis software such as IRAF.

There are many rules governing the exact format of keyword records so it is best to rely on a standard interface software like CFITSIO, IRAF or the IDL astro library to correctly construct or parse the keyword records rather than directly reading or writing the raw FITS file. There are a set of FITS conventions that have been defined to specify the physical, or world, coordinates to be attached to each pixel of an N-dimensional image.

1.10.2. The WCS Tool

The WCS tools are portable C utility programs and subroutines for setting and using the world coordinate system (WCS) of a FITS or IRAF image. The WCS describes the relationship between sky coordinates, such as right ascension and declination, and image pixels, and can be described using standard keywords in an image header.

The WCS links each pixel in an image to a specific direction in the sky. WCS tools provides software to fit a WCS to an image, find objects with known sky positions in an image, and find the sky positions of object discovered in an image. It also provides a variety of utilities to manipulate images and catalogs of astronomical objects. The subroutines on which it is based were originally developed to allow the display of sky coordinates while browsing image.

CHAPTER 02 LITERATURE REVIEW

In the late 19th century large-scale photographic spectroscopic surveys of stars were performed at Harvard College Observatory, producing spectral classifications for tens of thousands of stars, culminating ultimately in the Henry Draper Catalogue. In one segment of this work Antonia Maury included divisions of the stars by the width of their spectral lines. Hertzsprung noted that stars described with narrow lines tended to have smaller proper motions than the others of the same spectral classification. He took this as an indication of greater luminosity for the narrow-line stars, and computed secular parallaxes for several groups of these, allowing him to estimate their absolute magnitude. All these supergiant stars are too distant for meaningful parallaxes to have been measured before the advent of space astrometry, so no estimate of their absolute magnitude existed prior to that work. Russell's early (1913) versions of the diagram included these super-giants, those nearby stars with parallaxes measured at the time, and stars from the Hyades (a nearby open cluster), and several moving groups, for which the moving cluster method could be used to derive distances and thereby obtain absolute magnitudes for those stars.

2.1. Color Magnitude Diagram

There are several forms of the Hertzsprung–Russell diagram, and the nomenclature is not very well defined. All forms share the same general layout: stars of greater luminosity are toward the top of the diagram, while stars with higher surface temperature are toward the left side of the diagram.

The original diagram displayed the spectral type of stars on the horizontal axis and the absolute visual magnitude on the vertical axis. The spectral type is not a numerical quantity, but the sequence of spectral types is a monotonic ordered by stellar surface temperatures. Modern observational versions of the chart replace the spectral type by a color index (in diagrams made in the middle of the 20th Century, most often the B-V color) of the stars. This type of diagram is what is often called an observational Hertzsprung–Russell diagram, or specifically a color-magnitude diagram (**CMD**), and it is often used by observers. In cases where the stars are known to be at identical distances such as with a star cluster, the term color-magnitude diagram is often used to describe a plot of the stars in the cluster in which the vertical axis is the apparent

magnitude of the stars: for cluster members, by assumption there is a single additive constant difference between apparent and absolute magnitudes (the distance modulus) for all stars. Early studies of nearby open clusters (like the Hyades and Pleiades) by Hertzsprung and Rosenberg produced the first CMDs, antedating by a few years Russell's influential synthesis of the diagram collecting data for all stars for which absolute magnitudes could be determined.

Another form of the diagram plots the effective surface temperature of the star on one axis and the luminosity of the star on the other, almost invariably in a log-log plot. Theoretical calculations of stellar structure and the evolution of stars yield these quantities directly. This type of diagram could be called temperature-luminosity diagram, but this term is hardly ever used; when the distinction is made, this form is called the theoretical Hertzsprung–Russell diagram instead. A peculiar characteristic of this form of the H–R diagram is that the temperatures are plotted from high temperature to low temperature, which aids in comparing this form of the H–R diagram with the observational form.

Although the two types of diagrams are similar, astronomers make a sharp distinction between the two. The reason for this distinction is that the exact transformation from one to the other is not trivial. To go between effective temperature and color requires a color-temperature relation, and constructing that is difficult; it is known to be a function of stellar composition and can be affected by other factors like stellar rotation. When converting luminosity or absolute bolometric magnitude to apparent or absolute visual magnitude, one requires a bolometric correction, which may or may not come from the same source as the color-temperature relation. One also needs to know the distance to the observed objects (i.e., the distance modulus) and the effects of interstellar obscuration, both in the color (reddening) and in the apparent magnitude (extinction). For some stars circumstellar dust also affects colors and apparent brightness. The ideal of direct comparison of theoretical predictions of stellar evolution to observations thus has additional uncertainties incurred in the conversions between theoretical quantities and observations.

The CMD comprises four Main Regions:-

- White Dwarfs: very hot, the size of Earth, but not luminous

- Main Sequence stars are the size of the sun, various luminosities
- Red/Blue Giants are rare, very luminous stars
- Super giants are even more rare and even more luminous

2.1.1. Formation of Blue Stragglers

Several explanations have been put forth to explain the existence of blue stragglers. The simplest is that the blue stragglers formed later than the rest of the stars in the cluster, but evidence for this is limited. Another simple proposal is that blue stragglers are either field stars which are not actually members of the cluster to which they seem to belong, or are field stars which were captured by the cluster. This too seems unlikely, as blue stragglers often reside at the very center of the clusters to which they belong. Another theory is that blue stragglers are the result of stars that come too close to another star or similar mass object, causing stellar collision.

2.1.1. Evolution of Red Giant Stars

Red giants are evolved from main-sequence stars with masses in the range from about $0.3M_{\odot}$ to around $8M_{\odot}$. When a star initially forms from a collapsing molecular cloud in the interstellar medium, it contains primarily hydrogen and helium, with trace amounts of "metals" (in stellar structure, this simply refers to *any* element that is not hydrogen or helium i.e. atomic number greater than 2). These elements are all uniformly mixed throughout the star. The star reaches the main sequence when the core reaches a temperature high enough to begin fusing hydrogen (a few million kelvin) and establishes hydrostatic equilibrium. Over its main sequence life, the star slowly converts the hydrogen in the core into helium; its main-sequence life ends when nearly all the hydrogen in the core has been fused. For the Sun, the main-sequence lifetime is approximately 10 billion years. More-massive stars burn disproportionately faster and so have a shorter lifetime than the less massive stars

2.1.2. Formation of main Sequence Stars

When a proto-star is formed from the collapse of a giant molecular cloud of gas and dust in the local interstellar medium, the initial composition is homogeneous throughout, consisting of about 70% hydrogen, 28% helium and trace amounts of

other elements, by mass. The initial mass of the star depends on the local conditions within the cloud. (The mass distribution of newly formed stars is described empirically by the initial mass function.) During the initial collapse, this pre-main-sequence star generates energy through gravitational contraction. Upon reaching a suitable density, energy generation begins at the core using an exothermic nuclear fusion process that converts hydrogen into helium.

Once nuclear fusion of hydrogen becomes the dominant energy production process and the excess energy gained from gravitational contraction has been lost, the star lies along a curve on the Hertzsprung–Russell diagram (or HR diagram) called the standard main sequence. Astronomers will sometimes refer to this stage as "zero age main sequence", or ZAMS. The ZAMS curve can be calculated using computer models of stellar properties at the point when stars begin hydrogen fusion. From this point, the brightness and surface temperature of stars typically increase with age.

A star remains near its initial position on the main sequence until a significant amount of hydrogen in the core has been consumed, then begins to evolve into a more luminous star. (On the HR diagram, the evolving star moves up and to the right of the main sequence.) Thus the main sequence represents the primary hydrogen-burning stage of a star's lifetime.

2.1.3. The Ages of Clusters

To understand how stars evolve and change throughout their lifetimes, it is critical to know the properties of stars of different ages. Unfortunately, it is extremely difficult to determine the age of any random star. An old $1M$ ($M =$ mass of the sun) main sequence star looks nearly identical to a young $1M$ main sequence star, making it difficult to distinguish between them even if one is many giga years older than the other.

While it is difficult to measure the age of an individual star, it is relatively straightforward to measure the ages of a cluster of stars. If all of the stars in a cluster were born at the same time, then they share a common age. Thus, if the age of just one of the stars can be determined, then the age of all the stars will be known.

Fortunately, there is one class of stars for which it is quite easy to determine an age. Stars that have just used up the Hydrogen in their cores will begin to brighten, and will pull off the main sequence to higher luminosities. These stars are known as “turnoff” stars, because they are in the process of turning off the main sequence. Stars of different masses leave the main sequence at different times, because the main sequence lifetime of a star depends sensitively on the mass of the star. Thus, for a cluster of stars with similar ages, stars of only one particular mass will have just the right lifetime to be leaving the main sequence at the time the cluster is observed. Stars that are more massive than the “turnoff mass” will have already evolved into red giants or supergiant, and stars that are less massive will still be sitting comfortably on the main sequence.

To find the age of stars in a cluster, one therefore must identify the turn-off stars, and then estimate their masses. Identifying the turnoff stars is relatively straightforward. If one can find the main sequence stars in a cluster, the turnoff stars will be those that are just a bit brighter than the brightest stars that still lie firmly on the main sequence. To find the masses of the turnoff stars, one can use the fact that main sequence stars of a particular mass always have a particular temperature, and thus appear to have a particular color. Therefore, by measuring the color of the stars that are just now leaving the main sequence, one can estimate the mass of the turnoff stars. Since we know how long stars of any mass can live on the main sequence, we can therefore calculate how old the stars in a cluster might be. For example, suppose the turnoff stars in a cluster had the color of an A-star, which has a mass of 2 solar masses. A 2 solar mass star lives on the main sequence for roughly 1Gyr and thus the cluster must be around 1Gyr old. If the cluster were younger than 1Gyr, then there would still be stars more massive than 2M living on the main sequence. If the cluster was older, then all 2M stars would have already used up the Hydrogen in their cores and evolved far from the main sequence.

2.2. Distance Modulus

The distance modulus equation (1) is the difference between the apparent magnitude m (ideally, corrected from the effects of interstellar absorption and

atmospheric absorption) and the absolute magnitude M of an astronomical object. It is related to the distance d in parsecs by:

$$\mu = m - M \longrightarrow (1)$$

$$\log_{10} (d) = 1 + \mu/5 \longrightarrow (2)$$

$$\mu = 5 \log_{10} (d) - 5 \longrightarrow (3)$$

This definition is convenient because the observed brightness of a light source is related to its distance by the inverse square law (a source twice as far away appears one quarter as bright) and because brightness is usually expressed not directly, but in magnitudes.

Absolute magnitude M is defined as the apparent magnitude of an object when seen at a distance of 10 parsecs. Suppose a light source has luminosity $L(d)$ when observed from a distance of d parsecs, and luminosity $L(10)$ when observed from a distance of 10 parsecs. The inverse-square law is then written as:

$$L(d) = \frac{L(10)}{\left(\frac{d}{10}\right)^2} \longrightarrow (4)$$

The magnitudes and luminosities are related by:

$$M = -2.5 \log_{10} L(d) \longrightarrow (5)$$

$$M = -2.5 \log_{10} L(10) \longrightarrow (6)$$

Substituting and rearranging, we get:

$$m - M = 5 \log_{10}(d) - 5 = \mu \longrightarrow (7)$$

Which means that the apparent magnitude is the absolute magnitude plus the distance modulus.

Isolating d from the equation (7), we find that the distance (or, the luminosity distance) in parsecs is given by

$$5 \log_{10}(d) - 5 = \mu \longrightarrow (8)$$

$$D = 10^{\frac{\mu}{5} + 1} \longrightarrow (9)$$

The uncertainty in the distance in parsecs (δd) can be computed from the uncertainty in the distance modulus ($\delta\mu$) using

$$\delta d = 0.2 \ln(10) 10^{0.2\mu+1} \delta\mu = 0.461 d \delta\mu \longrightarrow (10)$$

Which is derived using standard error analysis.

2.3. Standardization

In order to find objective stellar apparent magnitudes, that is, a standard system, it is necessary to transform the obtained raw instrumental magnitudes, eliminating all the particularities of the measurement process. As said, this implies to consider the distortions introduced by the proper imaging system and by the atmosphere as well.

Therefore, the equations to be resolved are,

$$m_B = B + x_1(B) + x_2(B) * (B - R) + x_3(B) * X(B) \longrightarrow (11)$$

$$m_R = R + x_1(R) + x_2(R) * (B - R) + x_3(R) * X(R) \longrightarrow (12)$$

$$m_V = V + x_1(V) + x_2(V) * (B - R) + x_3(V) * X(V) \longrightarrow (13)$$

where:

m_B - the star's raw instrumental magnitude measured by the software on an image obtained through a standard B (blue) filter;

B - the star's true apparent magnitude measured through a standard B (blue) filter;

$x_1(B)$ - the constant offset between the arbitrary assigned instrumental magnitudes and the corresponding standard magnitudes for the standard B (blue) wavelengths;

$x_2(B)$ - the blue color term introduced by the used optical system, which accounts for its particular response at standard B (blue) wavelengths;

$x_3(B)$ - the blue airmass term, which accounts for the particular attenuation of the atmosphere regarding standard B wavelengths;

$X(B)$ - the airmass at the moment of the obtained image through the standard B filter;

All symbols are the same for every filter.

The usual way to resolve this system and find out the unknown terms is by also taking images of reference stars lying as close as possible to the stars going to be studied.

Reference stars means stars of known apparent magnitude values accepted as standards by the astronomical community. Those reference stars has been catalogued from high precision photometry works, such as those performed by ArloLandolt or Arne Henden. By far, the most used reference catalog is the one developed by Landolt, which not only employs the Johnson-Cousins color system filters, but has become the “practical definition” for the UBVRI standard system. The Landolt fields, as have been generically called, are a series of star regions near the celestial equator with well known magnitudes in at least the B, V and often R bands.

CHAPTER 03 MATERIAL AND METHODOLOGY

3.1. Material

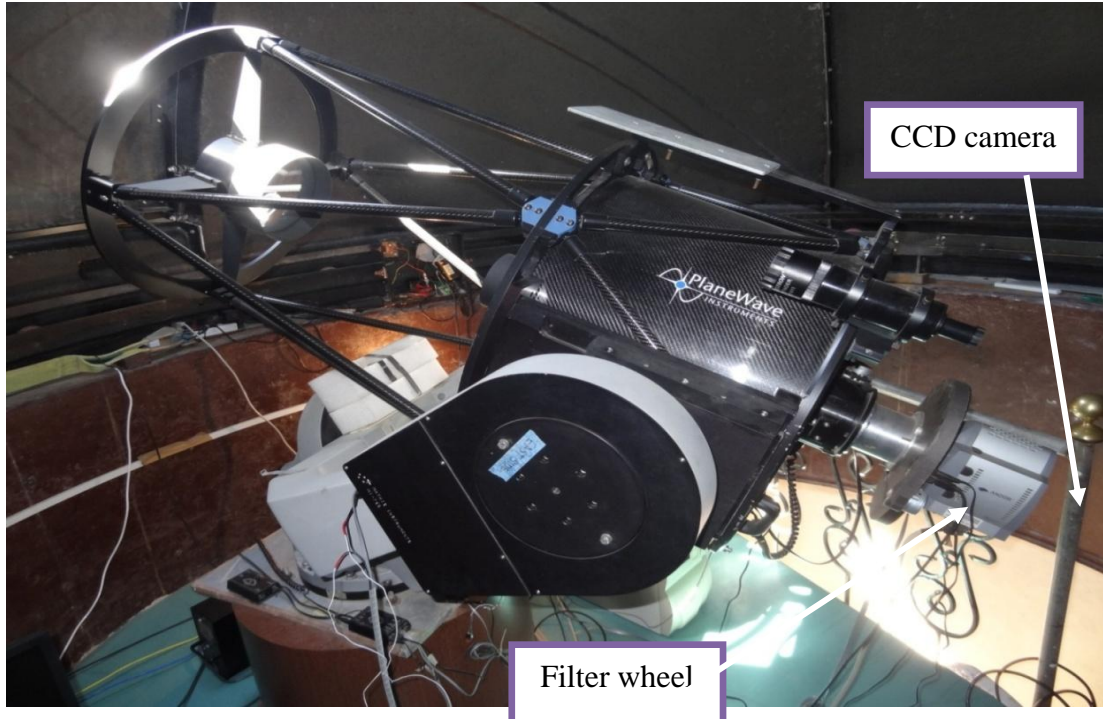


Figure 3.1 : 20 Inch Reflector Telescope

The Plane Wave Instrument CDK20 is a 20 inch (0.51 m) f/6.8 Corrected Dall-Kirkham Astrograph telescope. The CDK20 has a dual carbon-fiber truss design, with 3 cooling fans ejecting air from the back of the telescope. The CDK20 covers a 52 mm field of view without any field curvature, off-axis coma, or astigmatism. The instrument weight is 140 lbs (64 kg) and comes as a standard with a back plate retaining ring ready to accept the focuser of your choice.

The CDK (Corrected Dall-Kirkham) Optical Design is an innovative solution for an unsurpassed astro-imaging quality at an affordable price. The CDK telescope design provides excellent imaging with large format CCD cameras while retaining a high quality for visual use. The CDK design far exceeds the off-axis performance of most commercial telescope designs including the Ritchey-Chrétien design.

This no-compromise design is unique in making the optical alignment forgiving and collimation very easy. This guarantees the user the best possible performance from

the telescope. The end result at the image plane of the CDK design consists of no off-axis coma, no off-axis astigmatism and also a perfectly flat field (no off-axis defocus). The CDK design will enable you to pinpoint on stars from the center to the corner of the field of view.

3.1.1. Optical System

Table 3.1. features of optical system

| | |
|-----------------------------------|---|
| Aperture | 20 inch (508 mm) |
| Focal Length | 3454 mm (135.98 inch) |
| Focal ratio | F/6.8 |
| Central Obstruction | 39% of the Primary Mirror Diameter |
| Back Focus from Racked in Focuser | 5.8 inch (147 mm) |
| Weight | 140 lbs (63.5 kg) |
| OTA Length | 47 inch (1,194 mm) |
| Upper Cage | Carbon Fiber Truss |
| Lower Cage | Carbon Fiber Truss with Carbon Fiber Light Shroud |

3.1.2. Primary Mirror

Table 3.2 features of primary mirror

| | |
|-------------|---|
| Diameter | 20.5 inch (521 mm) |
| Aperture | 20 inch (508 mm) |
| Focal ratio | f/3 |
| Mounting | Laser Collimated and Permanently Fixed |
| Material | Precision Annealed Pyrex |
| Shape | Prolate Ellipsoid |
| Coating | Broadband AR Coatings (less than .5% reflected from 400 to 700nm) |

3.1.3. Secondary Mirror

Table 3.3 features of Secondary Mirror

| | |
|----------|---|
| Diameter | 7.5 inch (191mm) |
| Material | Precision Annealed Borosilicate |
| Shape | Spherical |
| Coating | Broadband AR Coatings (less than .5% reflected from 400 to 700nm) |

3.1.4. Lens Group

Table 3.4 Features of lens group

| | |
|------------------|---|
| Diameter | 90 mm (3.54 inch) |
| Number of lenses | 2 |
| Coating | Broadband AR Coatings (less than .5% reflected from 400 to 700nm) |

3.1.5. Standard Features

Table 3.5 Standard features

| | |
|---------------------------|--|
| Carbon Fiber Truss Design | Minimizes thermal expansion which causes the focus to shift with changes in temperature |
| Dovetail expansion joint | Allows for the difference in thermal expansion between carbon fiber and aluminum. The expansion joint allows the aluminum dovetail expand and contract without stressing the carbon fiber lower truss |
| Cooling Fans | Three cooling fans blow the optical tube pulling air through the telescope passing the primary mirror. This helps the telescope to reach thermal equilibrium quickly. The fans are controlled by a computer if the optional Electronic Focus Accessory (EFA Kit) is purchased. |

3.1.6. CCD camera

3.1.6.1. Function of the CCD camera

The highly sensitive detectors amplify the tiny current, which are generated by photons coming from faint objects. The light sensing ability of the CCD is only 2.5 millimeters on a side, but it contains 32,680 light sensitive photo sites. Each photo site consists of silicon substrata overlaid with an insulating layer of silicon dioxide and a strip of polysilicon above it. Within each line, the photo sites are separated by channel stops, a thin strip of silicon that has Boron atoms implanted. The channel stops block the movement of electrons across columns within the silicon.

When light fall a on the CCD, photons pass through the polysilicon and silicon dioxide layer into the silicon. They interact with atoms in the silicon crystal lattice, knocking electrons off the atoms according to the photoelectric effect. The number of electrons knocked free as such, is proportional to the number of oncoming photons. In a good CCD, about 60% of the incoming photons will knock out an electron. The electrons are trapped in potential wells, which are regions in the silicon layer where the electric potential is highest. Each photo site is a potential well. In electronic terminology, the swarm of electrons becomes a “charge packed” trapped in a potential well.

To read out the chip, the serial register is cleared and the imaging area is cycled once delivering one line’s worth of charge packets to the serial register. The line charge is then transferred to an amplifier. Once again the image area is cycled and the next line’s worth of charge packets enters the serial register. The process is repeated until every charge packet of every line is delivered to the amplifier.

3.1.6.2. Quantum Efficiency of the CCD

This is defined as the measurement of a device’s electrical sensitivity to light. It is the ratio of the number of photons detected by the camera to the number incident. That is the CCD doesn’t work with the same efficiency at every wavelength.

How CCD image spectra are processed

The quality of an image depends on the resolution of the sensor, which is measured by Megapixels. But raw CCD images are not perfect. Due to the digital nature of the data many of the imperfections can be compensated for or calibrated out of the final image through digital image processing. There are three signal components that consist of raw CCD images.

- Image signal – The image signal is produced by photons emitted from the source
- Thermal signal – The thermal signal produced (dark current thermal electrons) due to the thermal activity of the semiconductor material used in the CCD camera and this can be reduced by the cooling of the CCD to a low temperature
- Bias signal – The biased signal is the initial signal present in the CCD before exposing the CCD.

3.1.6.3. Photon Noise

The number of photons that reach the CCD while we are making an exposure varies randomly, just as we would expect the number of raindrops hitting a given patch of ground to vary during a rainstorm. Photon noise is produced due to the random fluctuations in the photon signal of the source. In other words the rate at which photons are received is not a constant. This may be due to environmental effects or the fluctuation of the production of photons itself.

3.1.6.4. Thermal Noise

Thermal noise occurs because the light-sensing photosets in the CCD chip generate a signal whether light falls on it or not. The warmer the CCD, the greater the non-light signal. Thermal effects are not constant

3.1.6.5. Readout Noise

Readout noise is the error in reading the signal and generally dominated by the on chip amplifier.

3.1.6.6.Quantized Noise

Quantized noise is the price we pay for having digital data. When the camera digitizes the output from the CCD chip, it divides the signal in to digital step.

3.1.6.7.Sensitivity Variation Noise

This will be the sensitivity variation from photosets to photosets the CCD detector or across the detector.

3.1.7. Specification of ANDOR CCD Camera

Table 3.6. Specification of ANDOR CCD Camera

| | |
|---------------------------------|---------------------|
| Active pixels(H×V) | 1024×1024 |
| Pixel size(W × H; μm) | 13×13 |
| Image area(mm) | 13.3×13.3 |
| Active Area Pixel Well Depth(e) | 80000 |
| Max readout Rate(MHz) | 30 |
| Frame rates(fps) | 26(full frame)-9690 |
| Read noise(è) | <1 with EM gain |
| E Max | >90% |



Figure 3.2 : ANDOR iXon Ultra camera

3.2.METHODOLOGY

1. Capture the real sky images with background stars using the CCD camera. The clusters were observed with the 20 inch reflector and Andor CCD camera. Around 10 frames of 5 second exposure from each filter were taken to stack the master frame. The master frame was used to analyze the star field.

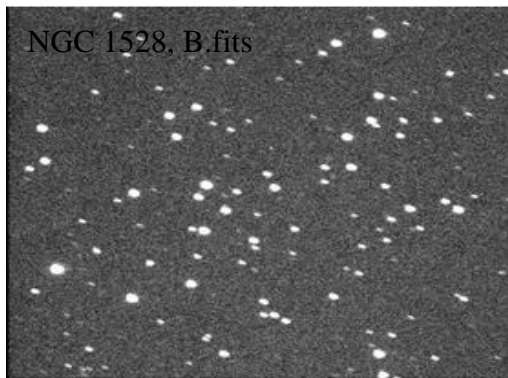
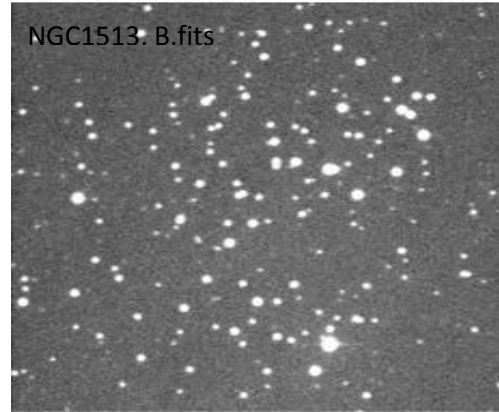
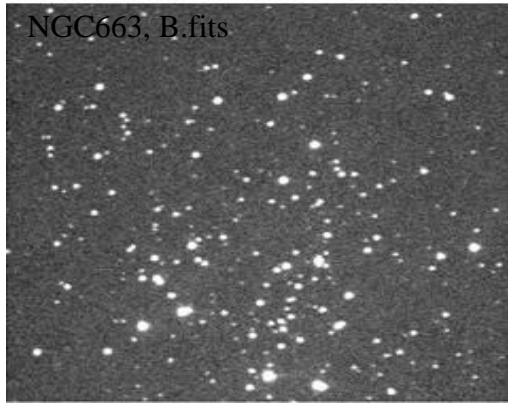


Figure 3.3. : cluster images

02. Corrections were done.

Due to the imperfections related to the change of filters and driving of the telescope some frames were blurred and distorted. Such images were removed before stacking to make the master frame.

03. Initially observed flat field images.

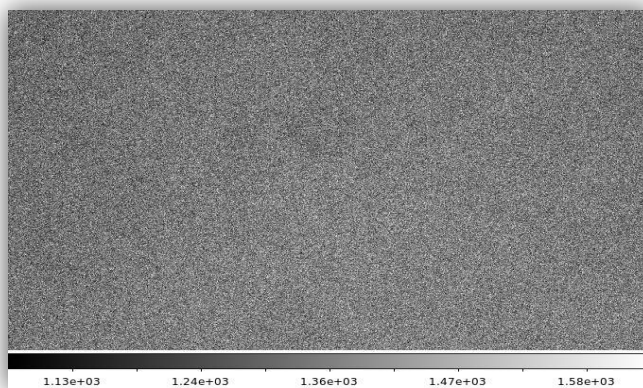


Figure 3.4 : flat field image

04. Images were categorized as U,B,V,R and I.

U,B,V,R and I are filters. Images were sent through these filters. So all images are categorized in terms of the filters.

```
list ="list name"  
  
while (fscan(list,s1)!=EOF){  
  
imgets((s1),"FILTA")  
  
s2=(imgets.value)  
  
print ((s1), >>(s2)//".list")  
  
print (s2)  
  
}
```

Figure 3.5. : image categorize code

Flat field correction

Flat-field correction is a technique used to improve quality in digital imaging. The goal is to remove artifacts from 2-D images that are caused by variations in the pixel-to-pixel sensitivity of the detector and/or by distortions in the optical path. It is a standard calibration procedure adopted in related instruments, from pocket digital cameras to giant telescopes.

Flat fielding refers to the process of compensation imposed for different gains and dark currents in a detector. Once a detector has been appropriately flat-fielded, a uniform signal will create a uniform output (hence flat-field). Then this means that any further signal is due to the phenomenon being detected and not due to a systematic error.

05. The cluster images were obtained and listed as V list, B list ,...

06. Master frames were made.

- First images were displayed
- Using imexamine ΔX and ΔY values were calculated.
- Using imshift images were shifted.

It is possible that the telescope is not tracking properly. It may also not be pointing correctly. Therefore after some time the field goes out of view. As such, the field has to be re-centered. Then the frames may not be perfectly aligned, and to realign we have to shift to a common center by 'imshift'.

```

                                I R A F
                                Image Reduction and Analysis Facility
PACKAGE = immatch
TASK = imshift

input =          R.fits Input images to be fit
output =         R Output images
xshift =        4.5875 Fractional pixel shift in x
yshift =        -0.96 Fractional pixel shift in y
(shifts_=       ) Text file containing shifts for each image
(interp_=      linear) Interpolant (nearest,linear,poly3,poly5,spline3,
(boundar=      nearest) Boundary (constant,nearest,reflect,wrap)
(constan=      0.) Constant for boundary extension
(mode =       ql)

```

Figure 3.6.: Parameters for imshift

07. After shifting the images all were recombined as one image.

In this case B filter image combine as B.fits and Vfilter images combine as V.fits.

```

                                Image Reduction and Analysis Facility
PACKAGE = immatch
TASK = imcombine

input =          *.fits List of images to combine
output =         V List of output images
(headers=       ) List of header files (optional)
(bp_masks=     ) List of bad pixel masks (optional)
(rejmask=      ) List of rejection masks (optional)
(nrejmas=     ) List of number rejected masks (optional)
(expmask=     ) List of exposure masks (optional)
(sigmas =     ) List of sigma images (optional)
(imcmb =      $I) Keyword for IMCMB keywords
(logfile=     STDOUT) Log file

(combine=      average) Type of combine operation
(reject =     none) Type of rejection
(project=     no) Project highest dimension of input images?
(outtype=     real) Output image pixel datatype
(outlimi=    ) Output limits (x1 x2 y1 y2 ...)
(offsets=     none) Input image offsets
More

                                ESC-? for HELP

```

Figure 3.7.: parameters for imcombine

08. This procedure was done for all cluster images of NGC663, NGC1513, NGC1528, and also for the standard star.

09. The correction for atmospheric and interstellar absorption.

In order to standardize the magnitudes, the atmospheric and interstellar absorptions have to be corrected. The parameter “airmass” is needed for this correction and the airmass of the observation site at the time of observation was calculated using the parameters RA, Dec, UT time. The image header was updated for the above parameters using the IRAF routine “hedit”.

- The ‘airmass’ was set for the entire three bands B,V and R.

The task ‘setairmass’ in the ‘astutil’ package will compute the effective ‘airmass’ of exposure, using the header values of RA, DEC, ST, EPOCH, and DATE-OBS. The task “setairmass” relies upon the header word OBSERSVAT to identify the observatory where the observations were made, and hence to decide on what latitude should be used in computing the ‘airmass’.

```

                                I R A F
                                Image Reduction and Analysis Facility
PACKAGE = astutil
  TASK = setairmass

images =B.fits Input images
(observa=      mountabu) Observatory for images
(intype =      beginning) Input keyword time stamp
(outtype=      effective) Output airmass time stamp

(ra  =         RA) Right ascension keyword (hours)
(dec  =         DEC) Declination keyword (degrees)
(equinox=      2000) Equinox keyword (years)
(st   =         ST) Local siderial time keyword (hours)
(ut   =         UT) Universal time keyword (hours)
(date  =       DATE-OBS) Observation date keyword
(exposur=      exptime) Exposure time keyword (seconds)
(airmass=      airmass) Airmass keyword (output)
(utmiddl=      utmiddle) Mid-observation UT keyword (output)
(scale  =       750.) The atmospheric scale height

(show  =        yes) Print the airmasses and mid-UT?
(update =        yes) Update the image header?
(overrid=      yes) Override previous assignments?
(mode  =        ql)

```

Figure 3.8.: Parameters for setairmass

10. Photometric analysis was applied to the clusters to obtain the instrumental magnitudes for clusters.

Run tasks NOAO, DIGIPHOT, DAOPHOT, EPAR and DAOFIND.

In these applications to let the standard deviation values display in relation to the images and run 'imexamine' it is necessary to put the cursor on background and press "m" and obtain the average values.

To get the FWHM displayed of the images and run 'imexamine' it is necessary to put the cursor on the star and press "r" and then obtain the average value. The aperture value is given by 3* FWHM.

```

      I R A F
      Image Reduction and Analysis Facility
PACKAGE = daophot
  TASK = daofind

image =      B.fits Input image(s)
output =    default Output coordinate file(s) (default: image.coo.?)
(starmap=   ) Output density enhancement image(s)
(skymap =   ) Output sky image(s)
(datapar=   ) Data dependent parameters
(findpar=   ) Object detection parameters
(boundar=   nearest) Boundary extension (constant|nearest|reflect|wra
(constan=   0.) Constant for boundary extension
(interac=   no) Interactive mode ?
(icomman=   ) Image cursor: [x y wcs] key [cmd]
(gcomman=   ) Graphics cursor: [x y wcs] key [cmd]
(wcsout =   logical) The output coordinate system (logical,tv,physica
(cache =    )_.cache) Cache the image pixels ?
(verify =   yes) Verify critical daofind parameters ?
(update =   no) Update critical daofind parameters ?
(verbose=    yes) Print daofind messages ?
(graphic=   stdgraph) Graphics device
(display=   stdimage) Display device
(mode =     ql)

```

Figure 3.9. : Parameters for daofind



Figure 3.10. :Image of selected stars using daofind , tvmark

Once the “phot” task runs, a flashing circle appeared on the selected stars in the display window allowing the coordinates and the corresponding magnitude to be measured in the ‘xgterm’ window. Then the measurements were shifted to the next star on this frame and proceeded until all the stars on this frame were measured. The next frame was displayed, and “phot” was run on it.

11. Standard star photometry was done for the PG0231, PG0918 and PG1047.

- The Standard Star Solutions

The standard stars photometry extracted the instrumental magnitudes for the standard stars. These instrumental magnitudes were transformed to the standard magnitudes which are in the IRAF database and thus enabled the determination of the absorption coefficients using the transformation equations. For this purpose the following steps were sequentially followed.

1. Create a catalog that contains the magnitudes and color indices of the standard stars on the standard system. A suitable catalog of the Landolt UBVRI standards was already available, and other “standard” standards catalogs may come on-line in the future; otherwise, the user will have to create his/her own.
2. Create a “standard star observations” file that consists of the airmass, instrumental magnitudes and errors for each set of observations (u,b, and v, say).
3. Create a file containing the algebraic form of the transformation equations, and references to indicate to which columns in the tables contain the necessary information. A sample template is available for making transformations using the Landolt catalog.

4. Fit the transformation equations; throwing out points to suit fancy. This step is done interactively, with lots of cool graphics, and should find it deeply satisfying.

After reducing the program stars, it is needed to then create a “program star observation file” that consists of the relevant instrumental magnitudes, airmasses, etc for each set of observations and finally you will then be able to apply the transformations to these data.

Transformation equations ;

$$r = r + \text{Const} + \text{Color Term} \times (B - R) + \text{Extinction} \times \text{Airmass}$$

$$b = B + \text{Const} + \text{Color Term} \times (B - V) + \text{Extinction} \times \text{Airmass}$$

$$v = V + \text{Const} + \text{Color Term} \times (B - V) + \text{Extinction} \times \text{Airmass}$$

Note that the instrumental magnitudes are on the left, and the standard magnitudes and indices are on the right; we are after the “best” values (in a least-squares sense) of each zero-point constant - “Const”, the color term coefficient, and the extinction coefficient. A few wrinkles to keep in mind: the airmasses are a little bit different for the “r”, “b”, and “v” exposures. Similarly the instrumental magnitudes will be “mB”, “mV”, and “mR”.

- Solving the above Transformation Equations

The task that actually solves the transformation equations is called fitparams. Edit the parameter file of this task until it resembles

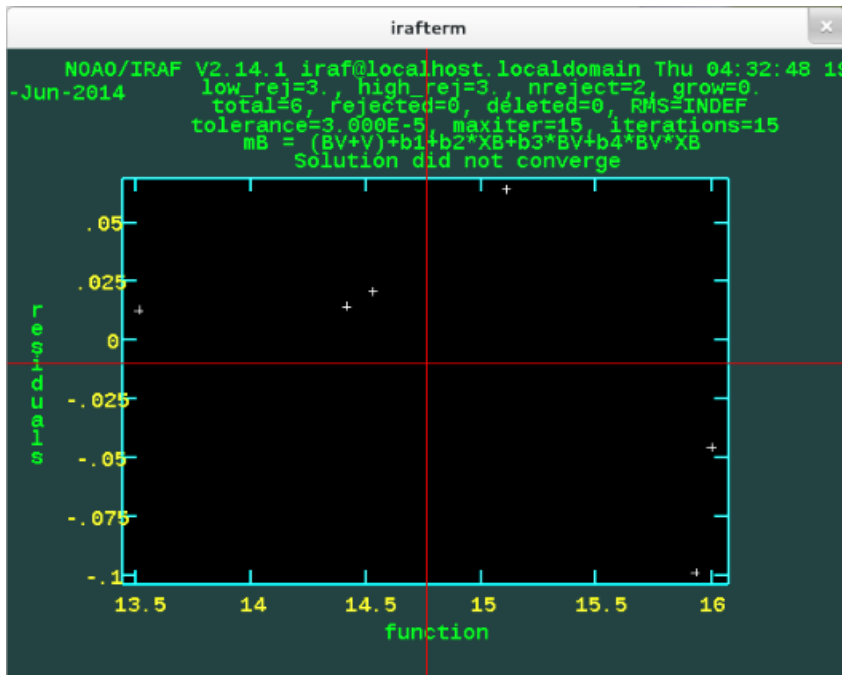


Figure 3.11 :Output of fitting graph by IRAF

- Transforming to the Standard System

Now we have a good instrumental magnitudes in all three filters.

Using transformation equations and coefficients transform the instrumental magnitudes to apparent magnitudes.

CHAPETR 4 RESULTS AND DISCUSSION

4.1. Results

4.1.1. NGC 663 (01:46:00 61:15:00)

Table 4.1. : Observation Air mass of the NGC 663 Open Cluster

| Filter | Air mass |
|--------|----------|
| B | 1.245 |
| V | 1.245 |
| R | 1.245 |

Table : 4.2. Instrumental magnitudes

| XCENTER | YCENTER | B mag | V mag | R mag |
|---------|---------|--------|--------|--------|
| 293.644 | 31.789 | 13.106 | 11.755 | 11.833 |
| 752.369 | 32.559 | 16.892 | 15.908 | 15.706 |
| 628.921 | 39.075 | 15.95 | 14.441 | 14.531 |
| 624.408 | 51.481 | 15.998 | 14.454 | 14.486 |

This is the way of instrumental magnitudes.

Table 4.3. : Standard solution of NGC663

| Parameters | Coefficient Values | Error |
|------------|--------------------|-------------|
| B1 | 2.577258 | 0.2681856 |
| B2 | -1.570808 | 0.2317329 |
| B3 | -0.1652877 | 0.03138015 |
| B4 | 0 | 0 |
| V1 | -2.425429 | 0.208744 |
| V2 | 2.378894 | 0.1800728 |
| V3 | 0.06378458 | 0.022532884 |
| V4 | 0 | 0 |
| R1 | 2.181621 | 0.1775197 |
| R2 | -1.12169 | 0.1524345 |
| R3 | 0.04766433 | 0.0416207 |
| R4 | 0 | 0 |

Table 4.4. : Absolute magnitude and Apparent magnitude

| Absolute V mag | Absolute (B-V) mag | Apparent V mag | Apparent B -V mag |
|----------------|--------------------|----------------|-------------------|
| -5.7 | -0.33 | 11.198 | 1.541 |
| -4.5 | -0.31 | 14.347 | 2.224 |
| -4 | -0.3 | 12.835 | 1.651 |
| -2.45 | -0.24 | 12.584 | 1.716 |
| -1.2 | -0.17 | 12.272 | 1.59 |

The instrumental magnitudes are transformed to apparent by the above coefficients.

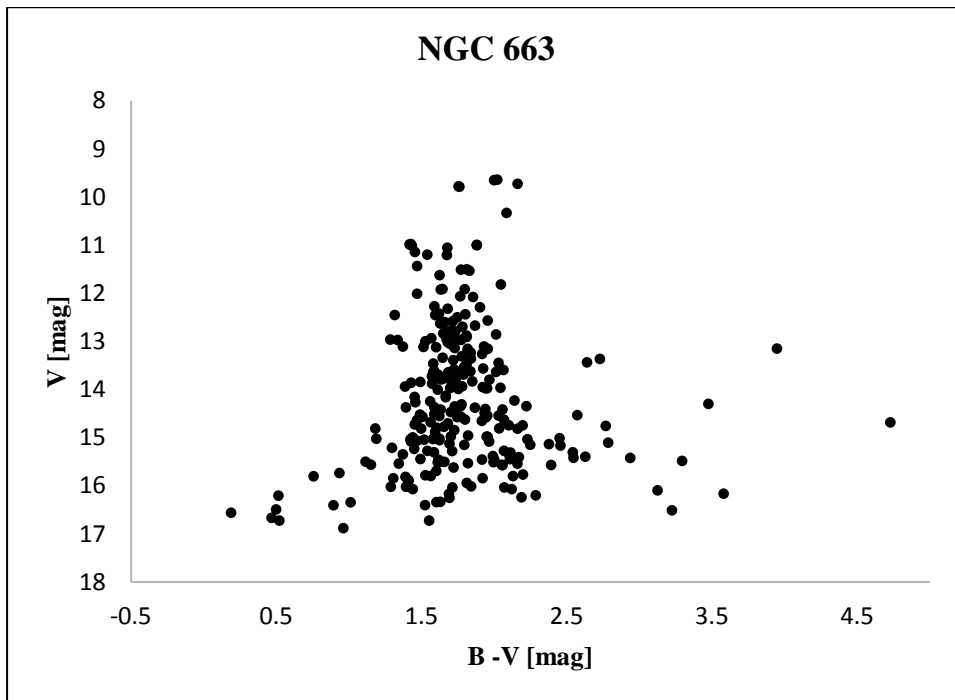


Figure 4.1. : CMD diagram of NGC 663

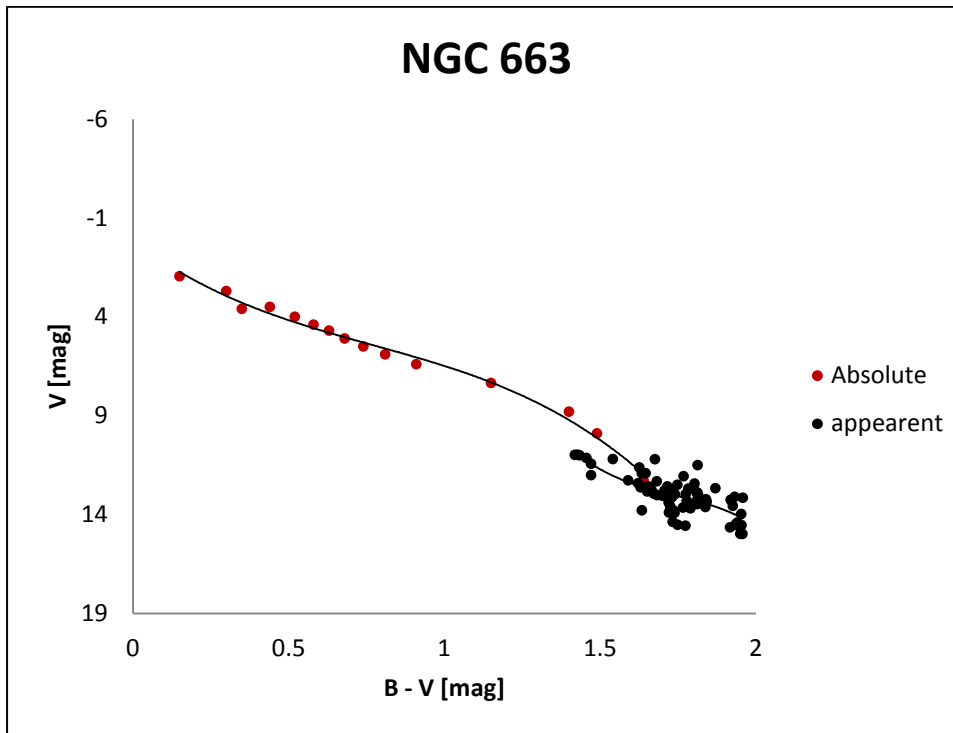


Figure 4.2. : CMD diagram of NGC663

This absolute magnitudes are not for the NGC663, these absolutes are for the nearby stars in the sky. But main sequence stars.

4.1.2. NGC 1513 (04:09:57,49:30:54)

Table 4.5. :Observation air mass of the NGC 1513 Open Cluster

| Filter | Air mass |
|--------|----------|
| B | 1.106 |
| V | 1.107 |

Table 4.6. : Instrumental magnitudes of NGC 1513

| XCENTER | YCENTER | B[mag] | V[mag] |
|---------|---------|--------|--------|
| 58.758 | 38.889 | 17.528 | 16.719 |
| 348.892 | 50.61 | 16.132 | 15.047 |
| 105.311 | 52.527 | 17.041 | 16.231 |
| 619.647 | 54.296 | 17.413 | 16.374 |

This is the way of instrumental magnitudes.

Table 4. 7. Standard solution for NGC 1513

| Parameters | Coefficient Values | Error |
|------------|--------------------|------------|
| B1 | 1.505286 | 0.05132937 |
| B2 | -1.234503 | 0 |
| B3 | -0.2389893 | 0.05834153 |
| B4 | 0 | 0 |
| V1 | -0.2151463 | 0.02033205 |
| V2 | -0.01289701 | 0 |
| V3 | 0.07160942 | 0.02278232 |
| V4 | 0 | 0 |

Table 4.8. : Absolute magnitude and Apparent magnitude

| M(B-V) | M _v | m _v | m(B-V) |
|--------|----------------|----------------|--------|
| 0.3 | 2.7 | 16.415 | 0.639 |
| 0.44 | 3.5 | 16.534 | 0.971 |
| 0.52 | 4 | 15.348 | 0.791 |
| 0.58 | 4.4 | 15.171 | 0.561 |

The instrumental magnitudes are transformed to apparent by the above coefficients.

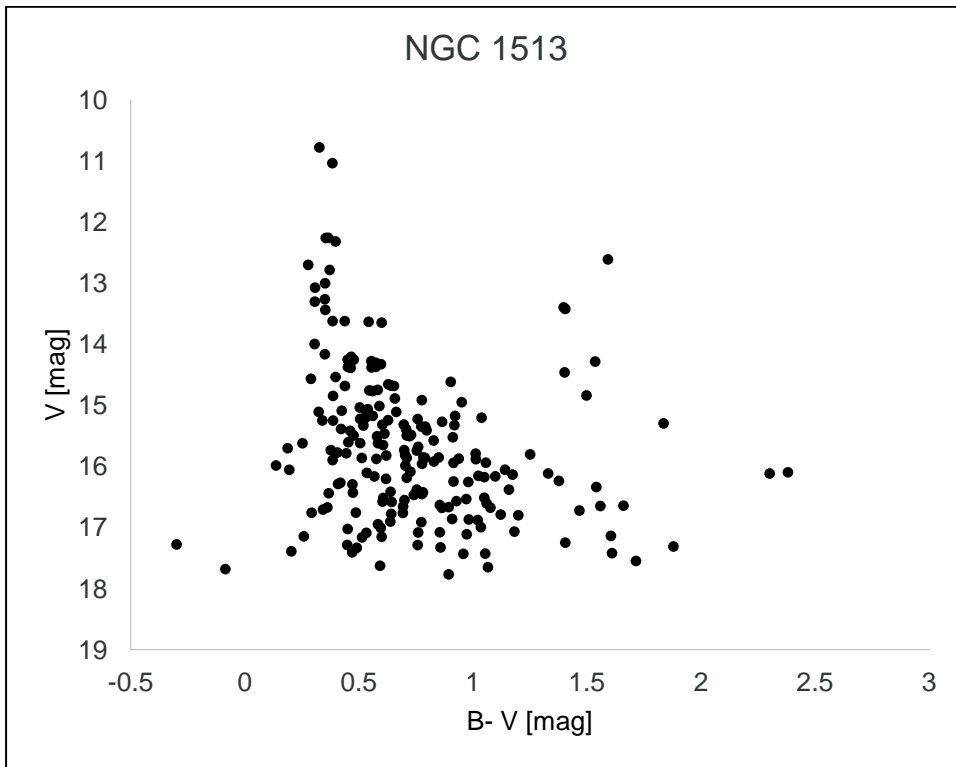


Figure 4.3. : CMD diagram of NGC1513

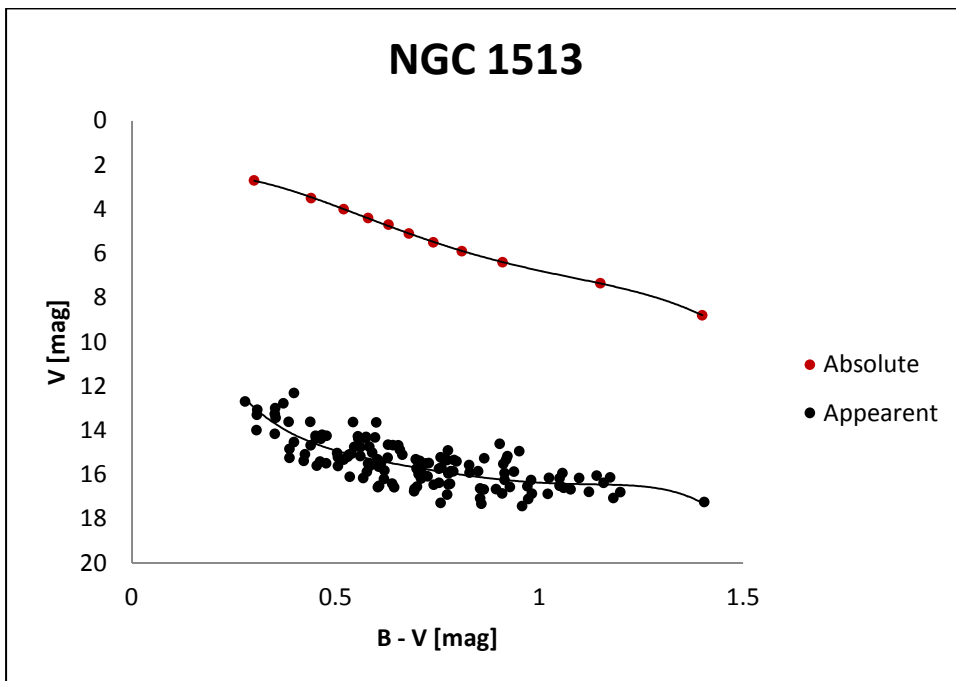


Figure 4.4. : CMD diagram of NGC 1513

This absolute magnitudes are not for the NGC663, these absolutes are for the nearby stars in the sky. But main sequence stars.

Table 4.9. : selected Absolute and Apparent magnitude for distance modulus

| mv | Mv | mv-Mv |
|------|-----|-------|
| 13.4 | 2.8 | 10.6 |
| 13.8 | 3 | 10.8 |
| 14.2 | 3.4 | 10.8 |
| 14.4 | 3.6 | 10.8 |
| 14.8 | 3.9 | 10.9 |
| 15 | 4 | 11 |
| 15.2 | 4.5 | 10.7 |
| 15.4 | 4.6 | 10.8 |
| 15.6 | 4.9 | 10.7 |

$$\text{Distance modulus} = (10.6+10.8+10.8+10.9+11+10.7+10.8+10.7)/9$$

$$= 10.7889 \text{ [mag]}$$

4.1.3. NGC 1528

Table 4.10. : Observation air mass of the NGC 1528 cluster

| Filter | Air mass |
|--------|----------|
| B | 1.198 |
| V | 2.207 |
| R | 1.201 |

Table 4.11. : Instrumental magnitudes of NGC 1528

| X center | Y center | Bmag | Vmag |
|----------|----------|--------|--------|
| 249.736 | 270.75 | 18.529 | 18.975 |
| 369.995 | 304.14 | 19.277 | 19.582 |
| 101.655 | 336.29 | 18.337 | 18.807 |
| 97.55 | 338.09 | 19.768 | 18.015 |

This is the way of instrumental magnitudes.

Table 4.12. : Standard solution of NGC1528

| Parameters | Coefficient Values | Error |
|------------|--------------------|------------|
| B1 | 2.577258 | 0.2681856 |
| B2 | -1.57080 | 0.2317329 |
| B3 | -1.1652877 | 0.03138015 |
| B4 | 0 | 0 |
| V1 | -2.425429 | 0.2087442 |
| V2 | 2.378894 | 0.1800728 |
| V3 | 0.06378458 | 0.02532884 |
| V4 | 0 | 0 |
| R1 | 2.181621 | 0.1775197 |
| R2 | -1.12169 | 0.1524345 |
| R3 | 0.04766433 | 0.0416207 |
| R4 | 0 | 0 |

Table 4.13 : The apparent magnitude of NGC 1528

| X center | Y center | V [mag] | B -V [mag] |
|-----------|----------|---------|------------|
| 900.634 | 23.591 | 19.188 | -1.145 |
| 490.506 | 28.606 | 15.12 | 1.559 |
| 0 661.234 | 28.698 | 16.228 | 1.022 |
| 1 485.983 | 30.536 | 15.001 | 1.602 |

The instrumental magnitudes are transformed to apparent by the above coefficients.

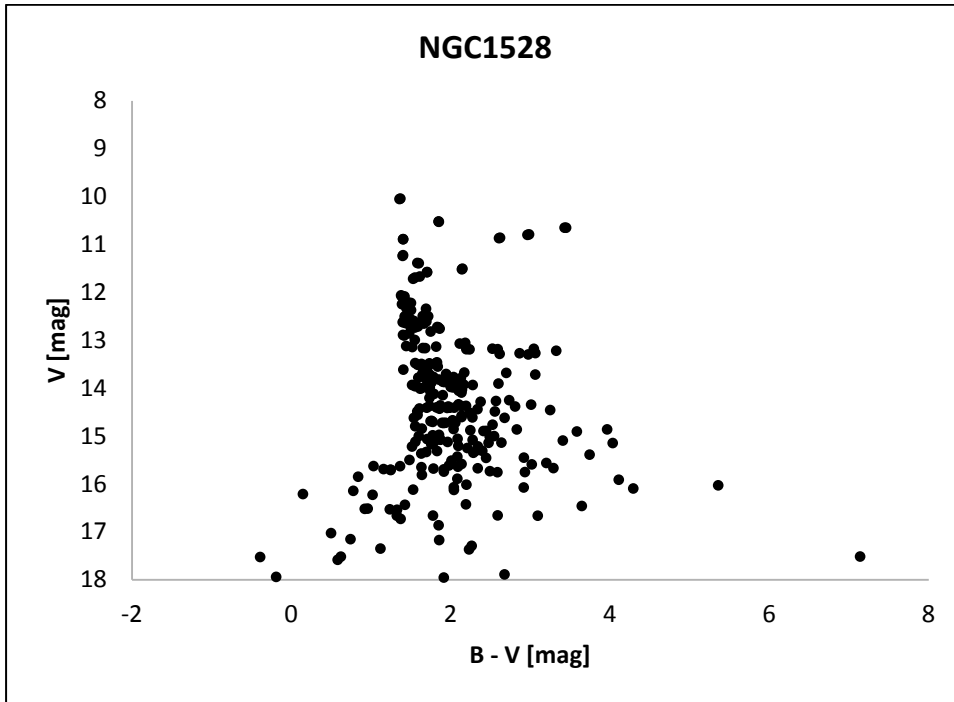


Figure 4.5. : CMD diagram of NGC1528

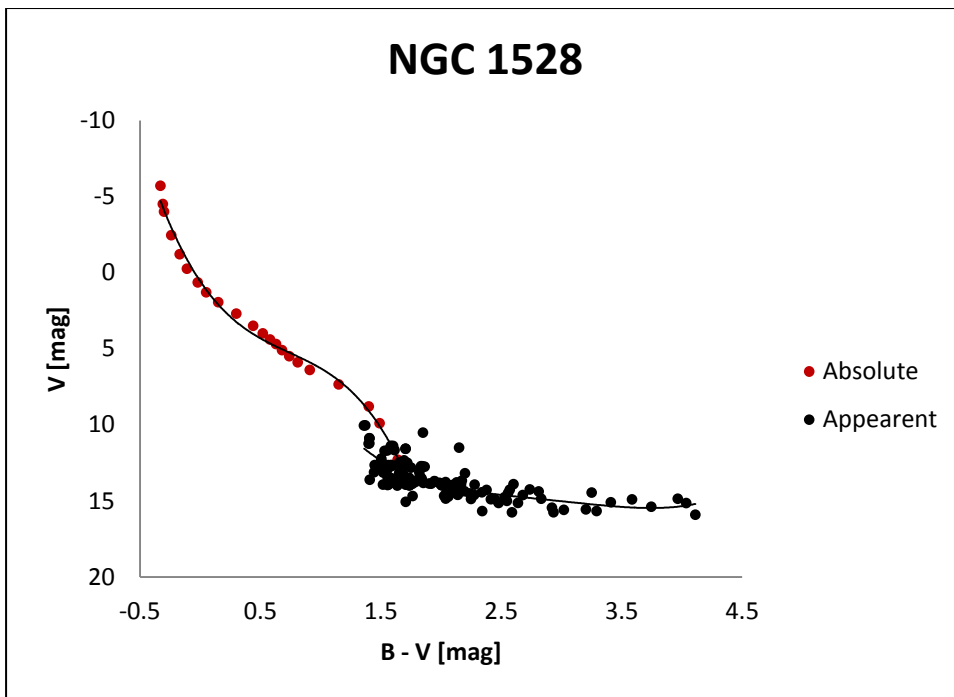


Figure 4.6. : CMD diagram of NGC1528

This absolute magnitudes are not for the NGC663, these absolutes are for the nearby stars in the sky. But main sequence stars.

4.2. DISCUSSION

The Color-Magnitude diagram of NGC663 showed a feeble main sequence pattern and also for the suspected red giant stars and white dwarfs.

The CMD diagram of NGC1528 has a strong main sequence branch with a prominent turn off point. The three stars (with RA and DEC values: 04:15:19.59, 51:14:23.03; 04:15:09.98, 51:11:40.98 & 04:15:46.57, 51:10:55.01) in NGC1528, which deviated from the main sequence, moving towards the red side can be confirmed as red giant stars. They also had white dwarfs.

The CMD diagram of NGC1513 has a main sequence branch with super giants and white dwarfs. In order to estimate the distance modulus, the CMD diagram of the open cluster NGC1513 was shifted to the standard CMD for nearby stars.

In the CMD diagrams of NGC663 and NGC1528 open clusters, the B-V range was shifted to the red side more than expected. Therefore it is inappropriate to do the shift to the absolute magnitude to determine the distance modulus. The standardization process produced higher V magnitudes which results the B-V term to deviate more to the red side in the CMD diagrams of the above two clusters. This may have resulted because of two reasons.

The interstellar reddening may lead to higher magnitudes for the red color than for the blue color for a stellar object. This is because the blue light is highly scattered by the interstellar medium than the red. Interstellar reddening occurs because interstellar dust absorbs and scatters blue light waves more than the red light waves, making stars appear redder than they are. This is similar to the effect seen when dust particles in the atmosphere of Earth contribute to red sunsets.

Though the interstellar reddening is corrected in the standardization process under the color term, this coefficient is not up to the expected value. On the other hand the standard stars observed for these two clusters were at very low altitudes and the 'airmass' coverage was not sufficient. Due to these reasons the CMD diagram of NGC663 and NGC1528 were deviated in B-V axis and hence could not obtain the distance modulus.

CHAPTER 05 CONCLUSION

- The Color-Magnitude diagram of NGC663 shows feeble main sequence patterns and suspected red giant stars.
- The CMD diagram of NGC1528 has a strong main sequence branch with a prominent turn off point.
- The distance modulus, $m_V - M_V$, is estimated to be 10.75 ± 0.995 in magnitude scale for the open cluster NGC1513.
- The stars in NGC1518 which deviate from the main sequence and moved to the red side can be conformed as red giant stars.

REFERENCES

- Arthur, c. N. "ALlen's Astrophysical Quantities." **4**: 390,391.
- G., P. (1996). "Variable Stars in the Young Open Cluster NGC 663." **46**: 357-360.
- I., B. K. A. D. L. (1960). "The open cluster NGC 1513." **4**: 313.
- van den Bergh, S. d. R., James (1978). "UBV Photometry of the Open Cluster NGC 663." **83**: 1075.
- van den Bergh, S. d. R., James (1978/09). "UBV photometry of the open cluster NGC 663."
- http://vizier.cfa.harvard.edu/viz-bin/VizieR?-6N&-out.form=H0&/**&-5N&%3C%22Label%22&catid%3D34630789&tabid%3D1&colid%3D7.
- <http://personal.inet.fi/surf/deepsky>.
- http://vizier.cfa.harvard.edu/viz-bin/VizieR?-6N&-out.form=H0&/**&-5N&%3C%22Label%22&catid%3D34630789&tabid%3D1&colid%3D7
- <http://adswww.harvard.edu/>.
- <http://www.noao.edu/education/arbse/arpd/oc>
- <http://simbad.u-strasbg.fr/simbad/sim-display?data=otypes>

Appendix I

IRAF Packages

noao - The NOAO optical astronomy packages

hedit - Header editor

hselect - Select a subset of images satisfying a boolean expression

imarith - Simple image arithmetic

imcombine - Combine images pixel-by-pixel using various algorithms

imdelete - Delete a list of images

imgets - Return the value of an image parameter as a string

imshift - Shift a list of 2-D images

display - Load an image or image section into the display

imexamine - Examine images using image display, graphics, and text

tvmark - Mark objects on the image display

cd - Change directory

cl - Execute commands from the standard input

eparam - Edit parameters of a task

delete - Delete a file or files (use IMDELETE to delete imagefiles)

head - Print the first few lines of a text file

phelp - Paged HELP: collects and pages the output of HELP

centerpars : Edit the centering algorithm parameters

Daofind : Find stars in an image using the DAO algorithm

Datapars : Edit the image data dependent parameters

Fitskypars : Edit the sky fitting algorithm parameters

Phot : Compute sky values and initial magnitudes for a list of stars

Photpars : Edit the aperture photometry parameters

Pdump : Print selected fields from a list of daophot databases